IEEE Photonics Journal
An IEEE Photonics Society Publication

Compact Brillouin Fiber Laser Based on Highly Nonlinear Fiber With 51 Double Spacing Channels

Volume 4, Number 4, August 2012

B. A. Ahmad
A. W. Al-Alimi
A. F. Abas
M. Mokhtar
S. W. Harun
M. A. Mahdi

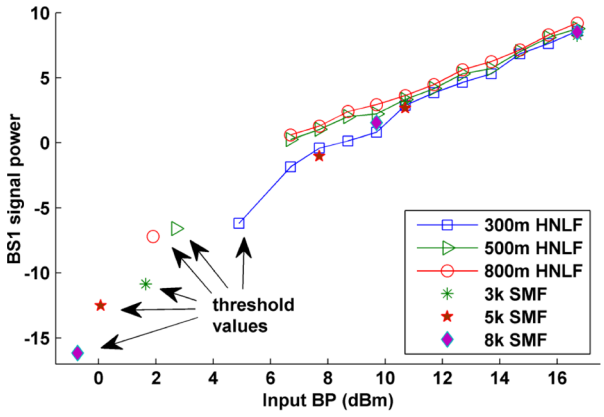

DOI: 10.1109/JPHOT.2012.2204970
1943-0655/$31.00 ©2012 IEEE

Compact Brillouin Fiber Laser Based on Highly Nonlinear Fiber With 51 Double Spacing Channels

B. A. Ahmad,[1,2] A. W. Al-Alimi,[1,2] A. F. Abas,[1,2] M. Mokhtar,[1,2] S. W. Harun,[3] and M. A. Mahdi[1,2]

[1]Centre of Excellence for Wireless and Photonic Networks, Engineering and Technology Complex, Universiti Putra Malaysia, Serdang 43400, Malaysia
[2]Photonics and Fiber Optic Systems Laboratory, Department of Computer and Communication Systems Engineering, Faculty of Engineering, Universiti Putra Malaysia, Serdang 43400, Malaysia
[3]Department of Electrical Engineering, University of Malaya, Kuala Lumpur 50603, Malaysia

DOI: 10.1109/JPHOT.2012.2204970

Manuscript received April 30, 2012; revised June 8, 2012; accepted June 12, 2012. Date of current version June 26, 2012. S. W. Harun acknowledges the University of Malaya for partial financial support under HIR-MOHE Grant D000009-16001. Corresponding author: B. A. Ahmad (e-mail: belalanwer@yahoo.com).

Abstract: A compact multiwavelength Brillouin fiber laser (BFL) with 51 stable double Brillouin frequency shift channels is demonstrated at room temperature. It uses a ring cavity with a 3-dB coupler for separation of odd-ordered and even-ordered Brillouin Stokes (BS) channels using a highly nonlinear fiber (HNLF) as the Brillouin gain medium. Compared with the use of a standard single-mode fiber, the HNLF-based BFL produces higher output power and a higher count of Stokes lines. At the maximum Brillouin pump (BP) power of 16.7 dBm, 36 odd channels and 15 even channels are generated with a channel spacing of 0.15 nm. The output power of the even channels is observed to be always lower than that of the odd channels as they are generated from the previous odd BS.

Index Terms: Nonlinear effect, Brillouin fiber laser, multiwavelength.

1. Introduction

Nonlinear effect phenomena in optical fiber have been experimented with to initiate multiwavelength generation in fiber lasers [1], [2]. Multiwavelength sources have attracted much interest in recent years, due to their low cost and many applications such as in dense wavelength division multiplexing (DWDM) communication systems, fiber sensing, optical component testing, photonic spectroscopy, optical sensors, and microwave photonics [3], [4]. To date, various techniques have been proposed for realizing multiwavelength laser. These techniques are mainly based on semiconductor optical amplifier (SOA), Erbium-doped fiber amplifier (EDFA), Raman amplifier [5], [6], and by exploiting stimulated Brillouin scattering (SBS) in optical fiber [7], [8]. Brillouin fiber laser (BFL) has an inherent advantage of fixed Stokes signal spacing, narrow linewidth and wide tuneability [9]. To increase the number of lasing Stokes, multiwavelength Brillouin Erbium fiber laser (MBEFL) has been proposed [10] in which both Brillouin and Erbium gains are utilized to initiate a Brillouin laser, as well as to assist in the cascading process. However, the wavelength tunability of MBEFL is limited since the Stokes and anti-Stokes generation are only efficient if the operation wavelength falls within the free-running Erbium-doped fiber laser bandwidth. At the same time, the wavelength spacing of the conventional MBEFL is approximately 10 GHz in the frequency domain, which is very narrow and thus difficult to be demultiplexed. Therefore, in an earlier work, Shee *et al.*

proposed MBEFL with double Brillouin spacing (~20 GHz), which has 10 output lines and a 9-nm tuning range within the C-band region [11]. In that setup, the MBEFL uses a four-port circulator to double the channel spacing by excluding the odd order signal Stokes and a piece of 6.7 km standard single-mode fiber (SSMF) as the gain medium. In another work, up to 15 Stokes lines with channel spacing of 0.154 nm and a 40-nm tuning range were produced using a figure of eight configuration and 2 km of highly nonlinear fiber (HNLF) as a nonlinear gain medium [12].

Recently, multiwavelength BFL has become more attractive due to its simpler configuration and wider tuning range [13], [14]. For instance, seven even ordered lines were obtained with 0.16 nm spacing by utilizing 100 m photonic crystal fiber (PCF) and figure of eight structure [15]. In a more recent work, 10 odd-ordered Stokes signals and 9 anti-Stokes signals with 0.17 nm wavelength spacing were obtained using 2.5-km SSMF as a Brillouin gain medium (BGM) assisted by a four-wave mixing (FWM) process [16]. In order to reduce the size of the device, nonlinearities must be enhanced in the gain medium, and hence, HNLFs have been used. This fiber is designed to enhance nonlinear coefficient without deteriorating the attenuation and thus provides a higher Brillouin gain for Stokes generation. In addition, the chromatic dispersion is tailored in the HNLF, which enhances a FWM process for anti-Stokes generation.

In this paper, a simple and compact new configuration is proposed to generate a multiwavelength BFL with double-spacing and two simultaneous outputs. The performance of the proposed BFL is investigated for two different gain media; HNLF and SSMF. The proposed new structure is able to generate a comb laser with the wavelength spacing of 0.154 nm and 0.17 nm. Up to 36 and 21 Stokes lines can be achieved by utilizing respectively HNLF and SSMF as a nonlinear gain medium. This is the first time that such achievement is reported to the best of our knowledge. Another advantage of this scheme is that it does not use any active gain medium in the cavity for amplification of pumping signals (Stokes and anti-Stokes lines). This greatly simplifies the system configuration.

2. Working Principle

The generation of multiwavelength BFL can be described as follows. The first-order Brillouin Stokes' signal (BS1) is initiated when the input Brillouin pump (BP) power exceeds the Brillouin threshold. It operates at a new wavelength which is Brillouin frequency shifted by 0.08 nm from the BP wavelength. The BS1 is split equally into two paths when passing through a 3dB optical coupler, one path toward optical spectrum analyzer 2 (OSA2) and the other path guides the Stokes line to oscillate inside the ring cavity to generate BFL. It is fed back into the BGM in the opposite direction of the input BP signal with Brillouin frequency down shifted by 0.08 nm from the BP wavelength to generate the second order Stokes signal (BS2) as the BS1 power exceeds the Brillouin threshold condition. BS2 undergoes another ~0.08 nm shift and oscillates in counter clockwise direction in the ring cavity to initiate the third-order Stokes signal in the opposite direction. The process continues until the power of higher-order Stokes signal becomes smaller and smaller and fails to exceed the Brillouin threshold condition. For this case, BS1 and all odd-ordered Brillouin Stokes (OS) signals, which are produced from the cascading process that propagates in clockwise (CW) direction move toward OSA1. However, BP, BS2 and all even-ordered Stokes' (ES) signals that propagate in counter clockwise (CCW) direction move toward OSA2. Because of the bidirectional propagations for BP and Brillouin Stokes (BS) signals inside the BGM, four-wave mixing (FWM) process is excited. The facing beams interact to form Stokes and anti-Stokes signals, which can be expressed as

$$w_{OS} = (w_P - \Delta w_B) - 2n\Delta w_B \quad (1)$$

$$w_{ES} = (w_p) - 2n\Delta w_B \quad (2)$$

$$w_{AOS} = (w_P) + \Delta w_B + 2n\Delta w_B \quad (3)$$

$$w_{AES} = (w_P + 2n\Delta w_B) \quad (4)$$

where Δw_B is the Brillouin downshift frequency from the BP frequency w_P, and $n = \{0, 1, 2, \ldots\}$. w_{OS}, w_{ES}, w_{AOS} and w_{AES} denote an OS, ES, odd-ordered anti-Stokes, and even-ordered

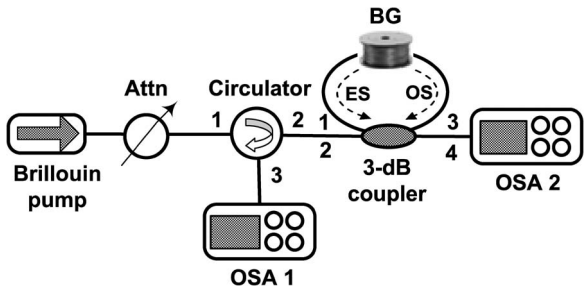

Fig. 1. Proposed configuration for multiwavelength BFL with double Brillouin frequency shift.

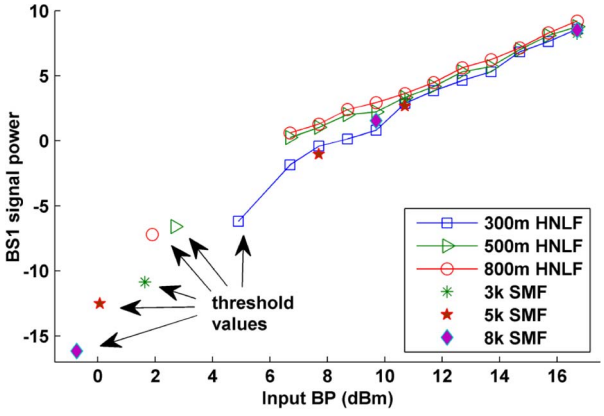

Fig. 2. Characteristics of BS1 power generated from different lengths and materials by varying input power.

anti-Stokes signals, respectively. The higher-order Stokes and anti-Stokes signals are initiated consecutively because of the cascaded SBS and multiple FWM processes.

3. Experimental Setup

Fig. 1 shows the proposed BFL with double-spacing multiwavelength output, where the cavity is based on a ring structure. The BP is an external tunable laser source (TLS) with a linewidth of approximately 200 kHz which is amplified by an EDFA to provide a sufficient output power. The BP power is controlled by an optical attenuator (Attn) that is injected into a BGM in the ring cavity through a 3-dB coupler via a 3-port circulator. The 3-port circulator has an insertion loss of 0.5 dB and an isolation of 53 dB. It is also used to route the backward propagating laser into an optical spectrum analyzer (OSA). A piece of HNLF (with three different lengths of 300 m, 500 m and 800 m) and SSMF (with three different lengths of 3 km, 5 km and 8 km) are tested as BGM for multi-wavelength generation. The HNLF has a nonlinear coefficient of $\sim$11.5 $W^{-1}km^{-1}$, effective area of $\sim$11.7 μm^2, attenuation of 0.82 dB/km, and cladding diameter of 125 μm. The BFL output spectrum can be measured by using two OSAs with resolution of 0.02 nm simultaneously in which the odd-ordered Stokes can be monitored at the port 3 of the circulator, while the even-ordered is monitored at port 4 of the 3-dB coupler as shown in Fig. 1.

4. Results and Discussion

Fig. 2 shows the BS1 output power against the input BP power for various lengths and types of BGM. In the experiment, the BP wavelength is fixed at 1561 nm and the BP power is varied from 0.7 dBm to 16.7 dBm. It is observed that the threshold power level for BS1 generation in both types of fiber decreases as the fiber length increases. The SBS threshold powers for the BFL configured

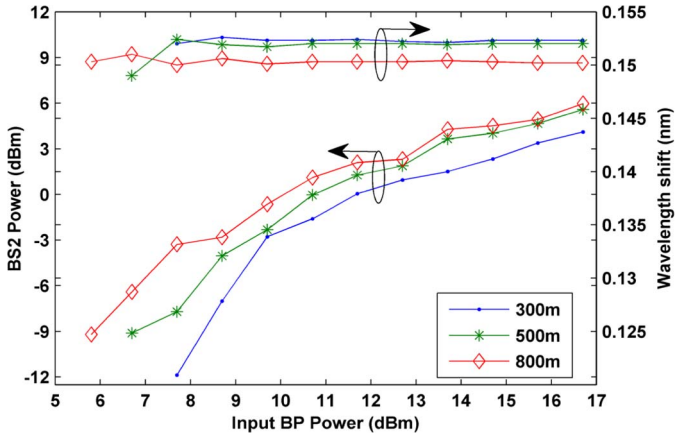

Fig. 3. Power characteristics of BS2 and wavelength shift from different lengths at different BP.

with 300 m, 500 m, and 800 m of HNLF are obtained at around 4.9 dBm, 2.7 dBm and1.9 dBm, respectively. Smaller thresholds of −0.74 dBm, 0.07 dBm, and 1.64 dBm are obtained with SSMF's lengths of8 km, 5 km, and 3 km, respectively. After the BP exceeds the threshold, BS1 power increases exponentially with the BP power. The maximum peak powers of BS1 are 8.5 dBm and 9.1 dBm at the maximum BP power of 16.7 dBm for 8 km long SSMF and 800 m long HNLF, respectively. The higher output power is observed with the HNLF due to the higher nonlinearity of the fiber, which provides a higher Brillouin gain and a smaller cavity loss due to a shorter BGM.

The increase in BS2 signal power and its wavelength shift are also investigated against BP power at various HNLF lengths as depicted in Fig. 3. BS2 is generated from BS1 power propagating in the opposite direction as the BP power exceeds the thresholds of 7.7 dBm, 6.7 dBm, and 5.8 dBm for HNLF lengths of 300 m, 500 m and 800 m, respectively. At the maximum BP power of 16.7 dBm, the peak powers of BS2 are obtained at 5.1 dBm and 2.1 dBm at the maximum HNLF length of 800 m and SSMF length of 8 km. The secondary axis of Fig. 3 illustrates the wavelength shift of BS2 against BP signal at various BP powers. The wavelength shift is fluctuating for spontaneous BS lines at BP power below the Brillouin laser threshold. However, the wavelength shifts are stable as the BP power is increased above the threshold power level. This phenomena can be explained as follows in which the Brillouin frequency shift (v_B) is represented by the following equation:

$$v_B = \frac{2n_P v_A}{\lambda_P} \tag{5}$$

where n_P is effective mode index and v_A is acoustic velocity through the gain medium at pump wavelength λ_P. It is shown that the Brillouin frequency shift is dependent on the fiber material having different n_p and v_A. Here, the output signals are shifted about $2v_B$ from the input signal, which is around 0.15 nm in HNLF and 0.17 nm in SSMF. This slight variation in frequency shift between the two fibers with different lengths is due to the difference in the effective refractive index, which is influenced by the fiber strain and the variation of strengths applied during spooling stage.

The output spectra of odd and even Stokes signals, which are measured by OSA1 and OSA2 for three different HNLF lengths, are shown in Fig. 4(a) and (b), respectively. In this experiment, the BP power and wavelength are fixed at 16.7 dBm and 1561 nm, respectively. As shown in the figure, both outputs show a comb spectrum with a double Brillouin frequency spacing of 0.15 nm. It is observed that the number of lines increases as the lengths of the fibers grow. For instance, 36 odd channels (21 Stokes and 15 anti-Stokes lines) and 15 even channels (9 Stokes and 6 anti-Stokes lines) are obtained at the longest fiber lengths of 800 m as shown in Fig. 4(a) and (b), respectively. The number of channels is higher as compared with another BFL with SSMF, which produces only 21 odd channels and 10 even channels, although the fiber length used is 10 times longer. This is attributed to the HNLF that has higher nonlinearity, which promotes SBS and FWM effects which

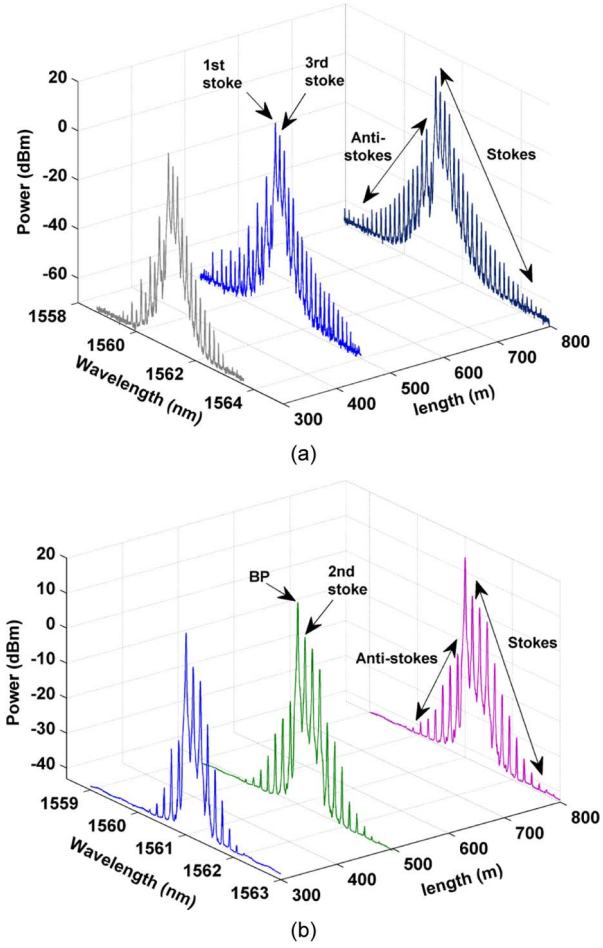

Fig. 4. Output spectra of the proposed multiwavelength BFL at three different lengths of HNLF: (a) odd channels and (b) even channels. (a) Odd channels observed at OSA1. (b) Even channels observed at OSA2.

assist the multiwavelength generation. The SBS process produces the first Stokes, which interacts with the pump beam to generate a new beam in anti-Stokes frequency through the FWM process. These beams again interact with each other to generate consecutive higher order Stokes and anti-Stokes via the Brillouin and FWM processes. Small peaks are also observed in between the channels due to Rayleigh scattering effect, which is back reflecting from the Stokes during propagation through the HNLF. For both types of fiber, subsequent Stokes lines always have lower power than the previous ones as they are generated from the previous Stokes signals. It is also observed that the background noise levels for Fig. 4(a) and (b) are slightly different. This is attributed to the cavity gain and loss in forward propagating direction which are different than those of the backward direction.

Fig. 5 illustrates the number of output lines generated by varying the input BP power from 6.7 dBm to 16.7 dBm as monitored by OSA1 and OSA2 simultaneously. When the BP power is less than 11.7 dBm, the number of lines is almost similar for both odd and even ordered Stokes signals. However, the signal power is different. For instance, with 500 m long HNLF and BP power of 7.7 dBm, the odd and even BS powers are obtained at 1.28 dBm and -10.4 dBm, respectively. A similar pattern is observed for the rest of Stokes signals power as the even BS is generated from the previous odd BS. For odd-ordered Stokes lines in Fig. 5, only those with signal power above the -60 dBm are counted, and for even-ordered Stokes lines only those above -40 dBm are

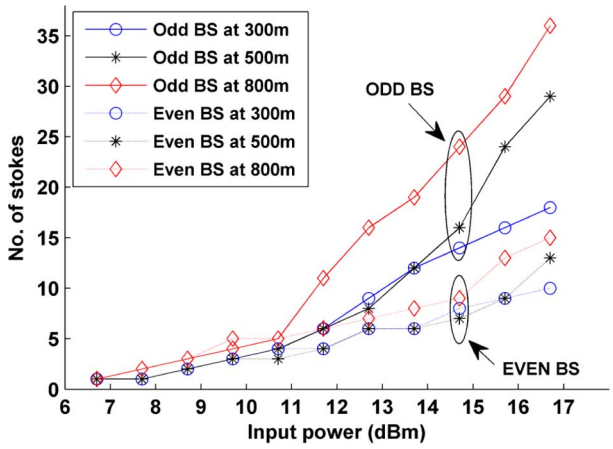

Fig. 5. Number of output lines against BP powers for both odd and even orders BS.

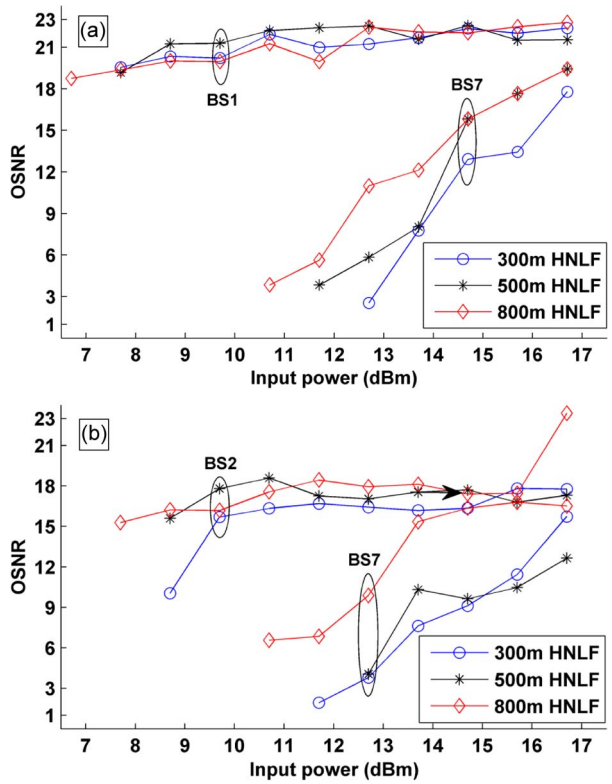

Fig. 6. OSNR against input BP powers for: (a) the odd-order BS (b) the even-order BS.

considered. Any channels below the reference levels are considered as a part of noise and cannot be utilized.

The optical signal to noise ratio (OSNR) is also investigated. In this paper, the OSNR for different length of HNLF as a function of BP power is measured for both odd and even ordered Stokes. Fig. 6 depicts the OSNR for selected signals. The OSNR improves as the BP power increases due to the increase in average signal power as compared to its noise. The highest OSNR is achieved at the first BS and then reduces for higher ordered Stokes. Since the loss increases with the length of the fiber, the OSNR is lower at longer fiber.

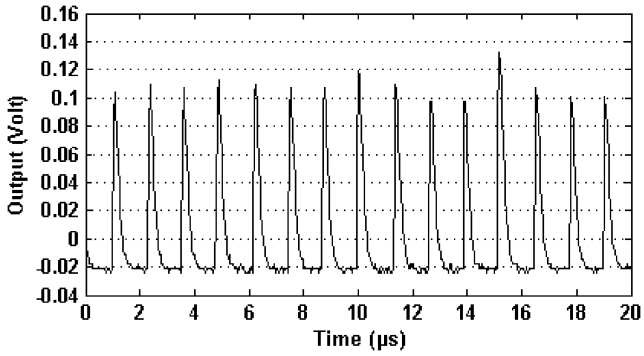

Fig 7. Oscilloscope trace of the output laser, recorded at BP power of 11 dBm.

A temporal behavior of the generated multiwavelength output is also experimentally investigated and the result is shown in Fig. 7. In the experiment, 500 m long HNLF is used as a gain medium. At the BP power of 11 dBm, a stable Q-switching pulses are obtained with *a* repetition frequency rate of 194.1 kHz and a pulse width of about 334 ns. The pulse generation is due to the growth of SBS, which causes a series of avalanche processes leading to Q-switching [17], [18]. The peak power of pulse is subject to fluctuation owing to SBS noise. The power fluctuation is approximately 10% in temporal domain and thus further investigations to improve the stability, and on the suitability of WDM system application are required, which is beyond the scope of this paper.

5. Conclusion

A compact multiwavelength BFL with double-Brillouin-frequency shift spacing was successfully realized and demonstrated. The lower order Stokes lines are initiated by SBS, while the higher order Stokes and anti-Stokes lines are initiated by multiple FWM process through simple ring cavity. In comparison to SSMF, HNLF based BFL produces a higher output power and number of Stokes. This is attributed to the fact that nonlinear effect is more pronounced in this fiber, which assists the multiwavelength generation through Brillouin scattering and four-wave mixing processes. The laser output also shows a Q-switching pulsation behavior with *a* repetition frequency rate of 194.1 kHz and pulse width of about 334 ns. The findings from this study will contribute toward the realization of the multiwavelength BFL as WDM light sources. In addition, this laser can be easily used in some future narrow-band microwave or as millimeter wave sources.

References

[1] Y. G. Han, T. Van Anh Tran, and S. B. Lee, "Wavelength-spacing tunable multiwavelength erbium-doped fiber laser based on four-wave mixing of dispersion-shifted fiber," *Opt. Lett.*, vol. 31, no. 6, pp. 697–699, Mar. 2006.
[2] N. S. Shahabuddin, H. Ahmad, Z. Yusoff, and S. W. Harun1, "Spacing-switchable multiwavelength fiber laser based on nonlinear polarization rotation and Brillouin scattering in photonic crystal fiber," *IEEE Photon. J.*, vol. 4, no. 1, pp. 34–38, Feb. 2012.
[3] J. Geng, S. Staines, and S. Jiang, "Dual-frequency Brillouin fiber laser for optical generation of tunable low-noise radio frequency/microwave frequency," *Opt. Lett.*, vol. 33, no. 1, pp. 16–18, Jan. 2008.
[4] F. Mihelic, D. Bacquet, J. Zemmouri, and P. Szriftgiser, "Ultrahigh resolution spectral analysis based on a Brillouin fiber laser," *Opt. Lett.*, vol. 35, no. 3, pp. 432–434, Feb. 2010.
[5] A. Halder, M. C. Paul, N. Shahabuddin, S. W. Harun, N. Saidin, S. S. A. Damanhuri, H. Ahmad, S. Das, M. Pal, and S. K. Bhadra, "Wideband spectrum-sliced ASE source operating at 1900 nm region based on a double clad Ytterbium-sensitized Thulium-doped fiber," *IEEE Photon. J.*, vol. 4, no. 1, pp. 14–18, Feb. 2012.
[6] M. Ummy, N. Madamopoulos, A. Joyo, M. Kouar, and R. Dorsinville, "Tunable multi-wavelength SOA based linear cavity dual-output port fiber laser using Lyot-Sagnac loop mirror," *Opt. Exp.*, vol. 19, no. 4, pp. 3202–3211, Feb. 2011.
[7] H. Ahmad, S. Shahi, and S. Harun, "Multi-wavelength laser generation with bismuth-based erbium-doped fiber," *Opt. Exp.*, vol. 17, no. 1, pp. 203–207, 2009.
[8] Z. Abd Rahman, M. Al-Mansoori, S. Hitam, A. Abas, M. Abu Bakar, and M. Mahdi, "Optimization of Brillouin pump wavelength location on tunable multiwavelength BEFL," *Laser Phys.*, vol. 19, no. 11, pp. 2110–2114, Nov. 2009.

[9] Z. A. Rahman, S. Hitam, M. Al-Mansoori, A. Abas, and M. Mahdi, "Multiwavelength Brillouin fiber laser with enhanced reverse-S-shaped feedback coupling assisted by out-of-cavity optical amplifier," *Opt. Exp.*, vol. 19, no. 22, pp. 21238–21245, Oct. 2011.
[10] A. Al Alimi, M. Al Mansoori, A. Abas, M. Mahdi, and M. Ajiya, "Optimization of tunable dual wavelength erbium doped fiber laser," *Laser Phys. Lett.*, vol. 6, no. 10, pp. 727–731, Oct. 2009.
[11] Y. Shee, M. Al-Mansoori, A. Ismail, S. Hitam, and M. Mahdi, "Multiwavelength Brillouin-Erbium fiber laser with double-Brillouin-frequency spacing," *Opt. Exp.*, vol. 19, no. 3, pp. 1699–1706, Jan. 2011.
[12] B. A. Ahmad, A. W. Al-Alimi, A. F. Abas, S. W. Harun, and M. A. Mahdi, "Stable double spacing multi-wavelength Brillouin-Erbium doped fiber laser based on highly nonlinear fiber," *Laser Phys.*, vol. 22, no. 5, pp. 977–981, Apr. 2012.
[13] M. Shirazi, M. Biglary, S. Harun, K. Thambiratnam, and H. Ahmad, "Bidirectional multiwavelength Brillouin fiber laser generation in a ring cavity," *J. Opt. A, Pure Appl. Opt.*, vol. 10, no. 5, p. 055101, May 2008.
[14] J. Tang, J. Sun, L. Zhao, T. Chen, T. Huang, and Y. Zhou, "Tunable multiwavelength generation based on Brillouin-Erbium comb fiber laser assisted by multiple four-wave mixing processes," *Opt. Exp.*, vol. 19, no. 15, pp. 14682–14689, Jul. 2011.
[15] R. Parvizi, H. Arof, N. M. Ali, H. Ahmad, and S. W. Harun, "0.16 nm spaced multi-wavelength Brillouin fiber laser in a figure-of-eight configuration," *Opt. Laser Technol.*, vol. 43, no. 4, pp. 866–869, Jun. 2011.
[16] J. Tang, J. Sun, T. Chen, and Y. Zhou, "A stable optical comb with double-Brillouin-frequency spacing assisted by multiple four-wave mixing processes," *Opt. Fiber Technol.*, vol. 17, no. 6, pp. 608–611, Dec. 2011.
[17] A. A. Fotiadi, P. Megret, and M. Blondel, "Dynamics of a self-Q-switched fiber laser with a Rayleigh-stimulated Brillouin scattering ring mirror," *Opt. Lett.*, vol. 29, no. 10, pp. 1078–1080, May 2004.
[18] A. A. Fotiadi and P. Megret, "Self-Q-switched Er-Brillouin fiber source with extra-cavity generation of a Raman supercontinuum in a dispersion-shifted fiber," *Opt. Lett.*, vol. 31, no. 11, pp. 1621–1623, Jun. 2006.